J|A|C|S COMMUNICATIONS

Published on Web 07/30/2010

Visualization of a Discrete Solid-State Process with Steady-State X-ray Diffraction: Observation of Hopping of Sulfur Atoms in Single Crystals of Realgar

Panče Naumov,*[,†,‡] Petre Makreski,[‡] Gjorgji Petruševski,[‡,§] Tomče Runčevski,[‡] and Gligor Jovanovski[‡,||]

Department of Material and Life Science, Graduate School of Engineering, Osaka University, 2-1 Yamada-oka, Suita, Osaka 565-0871, Japan, Institute of Chemistry, Faculty of Science, SS. Cyril and Methodius University, Arhimedova 5, 1000 Skopje, Macedonia, Research and Development Institute, Alkaloid AD, Aleksandar Makedonski 12, 1000 Skopje, Macedonia, and Macedonian Academy of Sciences and Arts, Bul. Krste Misirkov 2, 1000 Skopje, Macedonia

Received April 12, 2010; E-mail: npance@wakate.frc.eng.osaka-u.ac.jp

Abstract: A molecular movie showing migration of a sulfur atom between molecules of realgar (α-As_4S_4) was obtained by a series of structure determinations of the dark stage of this all-solid autocatalytic reaction set.

In view of the need to understand the structural/energetic factors that determine the outcome of a solid-state photochemical reaction or a physical process at an atomic level, direct monitoring of the temporal reaction course stands at the frontier of current structural research. If the single-crystal integrity is retained during the reaction, the mechanism and dynamics of a slow chemical reaction can be conveniently studied by determining the three-dimensional structure using steady-state X-ray diffraction (XRD) analysis at consecutive time points that are typically separated by hours.[1] On the other hand, accurate geometrical facets of very fast processes (down to the picosecond time scale) following excitation can be observed with ultrafast time-resolved XRD.[2] A prerequisite for stepwise analysis of the reaction mechanism for the process of interest in each case is its gradual course (on the respective time scale), that is, kinetics that is *slow* relative to the time interval at which the process is being probed. Herein, we report experimental evidence of a *fast* and *discontinuous* photoinduced process obtained by steady-state single-crystal XRD: migration of a sulfur atom during the photoinduced transformation of the molecular inorganic solid realgar (α-As_4S_4) into its isomer pararealgar. We anticipated that the extremely rare combination of solid-state cooperativity and balanced thermochemistry would turn the dark stage of this reaction into a phototriggered *autocatalytic reaction set*.[3] Similar reaction sets are known in the life sciences[4] and nonlinear chemical dynamics in solution,[5] and a recent report on a [4 + 4] photodimerization has provided the first example of solid-state autocatalysis with an organic compound.[6] To our knowledge, the photoinduced isomerization of realgar is the only known example of an inorganic all-solid system with self-sustainable dynamics. Moreover, this appears to be the first case where the solid-state isomerization is initiated with atmospheric oxygen.

Realgar absorbs visible photons with energies in the range 1.85−2.48 eV,[7] with the absorption peaking at the bandgap, 2.40(5) eV,[8] whereby it irreversibly isomerizes to pararealgar, in which

Scheme 1. Reaction Mechanism Based on Light (eqs 1 and 2) and Dark [eqs 3 and 4 (=2)] Stages Suggested for the Photoinitiated Rearrangement of Realgar to Pararealgar via Uzonite

$$5As_4S_4(\text{realgar}) + 3O_2 + h\nu \rightarrow 4As_4S_5(\text{uzonite}) + 2As_2O_3 \quad (1)$$

$$As_4S_5(\text{uzonite}) \rightarrow As_4S_4(\text{pararealgar}) + S \quad (2)$$

$$\alpha\text{-}As_4S_4(\text{realgar}) + S \rightarrow As_4S_5(\text{uzonite}) \quad (3)$$

$$As_4S_5(\text{uzonite}) \rightarrow As_4S_4(\text{pararealgar}) + S \quad (4)$$

the positions of one arsenic atom and one sulfur atom in the As_4S_4 cluster have been exchanged.[9] A four-step mechanism based on initiation by aerobic photooxidation and subsequent propagation, as outlined in Scheme 1, was postulated for this reaction.[10−13] Unlike β-As_4S_4,[14] which isomerizes gradually, the reaction of α-As_4S_4 is a discontinuous process; the sharp change in the cell volume has been attributed to rupture of one of the As−S bonds, but the crystal disaggregation occurring with continuously excited specimens has to date obscured monitoring of the reaction beyond the initial stages.

Recently, we noticed that once very small red crystals of realgar are exposed to direct visible light, they convert slowly to a yellow powder of pararealgar, and the process continues even after they have been stored in the dark (see the Figure 1a inset). Because the leaving sulfur atom (eq 4) is effectively being "reused" in a reaction with another realgar molecule (eq 3), we anticipated that providing

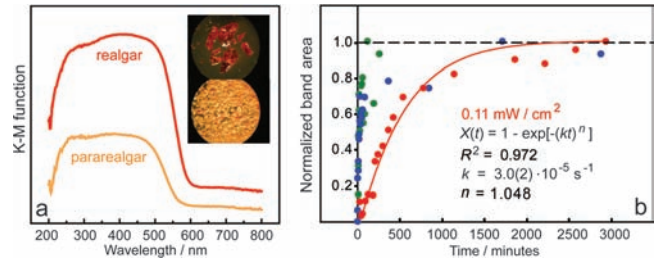

Figure 1. (a) UV−vis spectra of realgar and pararealgar (shown in the inset), powdered and diluted with NaCl (1%), recorded in reflectance mode. (b) Temporal profiles and kinetic constants of the conversion of realgar to pararealgar induced by excitation at 1.96 eV and monitored by the reaction extent, expressed as the normalized integrated intensity of the 274 cm^{-1} Raman band of pararealgar (green, blue and red marks correspond to excitation at 1.81, 0.77 and 0.11 mW cm^{-2}, respectively). The red line in (b) represents the kinetic curve fitted to the excitation with the lowest power density (0.11 mW cm^{-2}) according to the JMAK model.

† Osaka University.
‡ SS. Cyril and Methodius University.
§ Alkaloid AD.
|| Macedonian Academy of Sciences and Arts.

10.1021/ja1030672

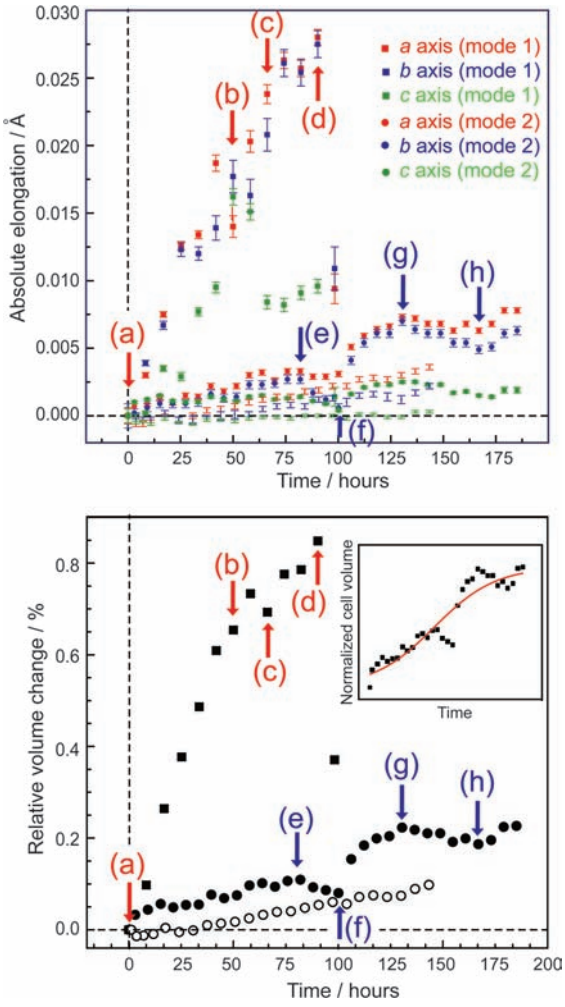

Figure 2. Temporal profiles of (top) the absolute axis elongation and (bottom) the relative change in the cell volume of realgar single crystals recorded in mode 1 (■) and mode 2 (●). Marks having only vertical bars in the upper panel and the open circles in the lower panel correspond to a control series (nonexcited sample). The inset shows a fit of the mode 2 data with the Prout−Tompkins kinetic model.

a steady input of the reactant would result in self-sustainability of the two dark-stage reactions (eqs 3 and 4).[15] Moreover, the close packing[9] was expected to provide conditions for cooperative action during the spatial progression, and thus, large yields could ideally be expected at a minimum excitation.

To evaluate the effect of excitation on the reaction kinetics, microcrystals of realgar[16] were continuously excited with continuous-wave (cw) laser light at 1.96 eV, and the dependence of the conversion on the excitation power density was monitored through the integrated intensity of the nearly pure Raman mode (89% S−As−S bending) of pararealgar at 274 cm^{-1} as a reporter band[17] [Figure 1b; also see Table S1 and Figure S1 in the Supporting Information (SI)]. The excitation densities of 0.11, 0.77, and 1.81 mW cm^{-2} showed that the kinetics could easily be controlled by varying the intensity of the incident light, and the reaction rate could be conveniently adjusted to collect complete XRD data sets at a desired number of time points during the course of the reaction.

The role of each stage in this rearrangement was studied by two series of XRD experiments. In the first series (mode 1), the light and dark reactions were conducted simultaneously by continuous excitation of a single crystal (2.33 eV) with very weak cw light (~3 μW cm^{-2}). In the second series (mode 2), which was designed to study the dark stage alone, a crystal was first excited (600 s; 0.1

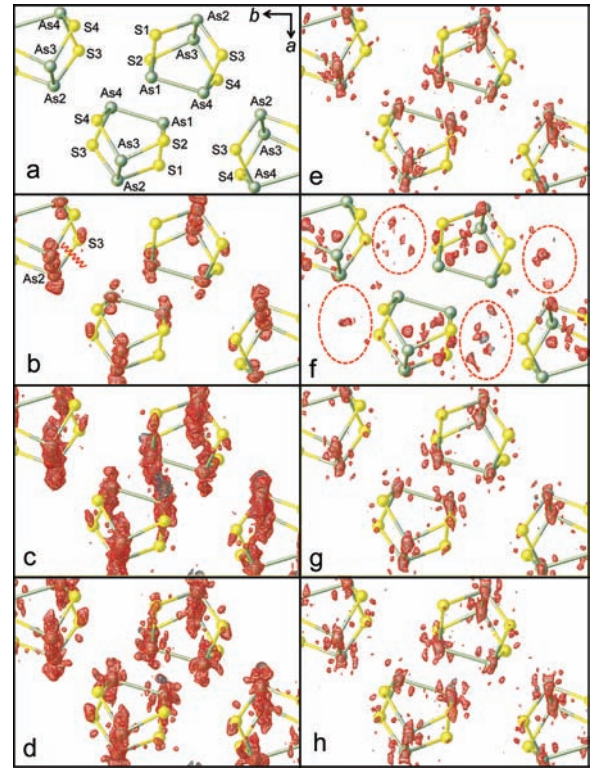

Figure 3. Snapshots showing the change in the difference electron density ($F_{obs} - F_{calcd}$) in the unit cell of realgar (viewed along the *c* axis) taken at the points marked in Figure 2. The positive residual electron density is plotted at (a−d) 2.0 and (e−h) 1.2 e $Å^{-3}$. Color codes: As, gray; S, yellow.

mW cm^{-2}), and subsequently the structure was probed in the dark.[18] In mode 1, the cell expanded strongly during the course of 90 h, mostly along the *a* and *b* axes (~0.028 Å), before disintegration occurred at $t \approx 100$ h [point (d) in Figure 2]. The *c* axis expanded for 58 h, but it shrank and remained constant afterward. We were surprised to see that in mode 2, when only the dark reaction could proceed, the cell also showed a small but significant expansion (mostly along *a* and *b*) during the first 82 h ($\Delta V = +0.87$ $Å^3$), after which it shrank at a time point close to that of the disintegration in mode 1 ($t = 94-100$ h). This observation conforms to the understanding based on eqs 1−4 that two of the reactions (eqs 3 and 4) occurring in continuously excited crystals proceed with a smaller yield even in the dark. A second surprise to us was the observation that after being aged in the dark for 100 h [point (f) in Figure 2], the crystal underwent sudden *expansion* ($\Delta V = +1.63$ $Å^3$), although its integrity was sustained.

Movies S1 and S2 in the SI show the sequential changes in residual electron density in each mode, and Figure 3 contains selected snapshots at the points marked in Figure 2. The reaction commences at sulfur atom S3 by rupture of the As2−S3 bond. In mode 1, between the time points (a) and (b), the realgar molecule ($V/Z = 199.94$ $Å^3$)[19] is distorted within the *ac* plane, and the cell expands because uzonite ($V/Z = 227.19$ $Å^3$)[20] is produced. The expansion continues between points (b) and (c), but the cell now shrinks along the *c* axis with the volume remaining nearly constant thereafter. At point (c), excess electron density appears around S1. The volume remains nearly constant up to point (d), where the maximum yield of uzonite has been reached, with the shrinkage along the *c* axis compensating for the small expansion along *a* and *b*. At point (d), the cell shrinks abruptly as a result of uzonite depletion due to the conversion to pararealgar ($V/Z = 201.71$ $Å^3$),[21] which ultimately triggers crystal disintegration.

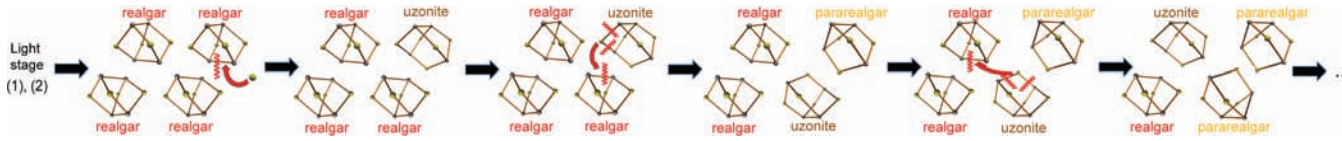

Figure 4. Cartoon of the mechanism of the dark phase in the photoinitiated rearrangement of realgar to parearealgar. It should be noted that this is a simplified representation and does not represent the actual molecule disposition in the unit cell, which is presented in Figure 3. Color codes: As, gray; S, yellow.

In mode 2, after the initial excitation, the volume expands because of the limited amount of products (Figure 2, bottom panel). Reactions 3 and 4 proceed autocatalytically, and the cell expands slightly up to point (e) ($t \approx 80$ h), which is close to point (d) of the light phase ($t \approx 85$ h). After point (e), the uzonite transforms into parearealgar, and the cell shrinks up to point (f). Beyond point (f), the cell expands again because the released sulfur atoms react with the remaining realgar molecules, yielding uzonite (eq 3). The production of uzonite is maximal at ~130 h [point (g)] and decreases afterward as a result of decay of uzonite to parearealgar (eq 4).

The most remarkable feature in mode 2 is the sharp change in the electron distribution at point (f), where excess density appears in the intermolecular region (Figure 3f). A control experiment (Figure 2) confirmed that this event is not a result of X-ray-induced effects but is due to the self-sustained autocatalytic process. The effect appears in mode 1 as well as in mode 2, although in the former case it is much more enhanced because of the steady excitation and drives the crystal disintegration. In mode 2, the cell expansion is smaller, which explains why the crystal integrity is sustained. Because this process is related to the light stage (eqs 1 and 2), it can be concluded that it represents hopping of the sulfur atom between the molecules of uzonite and realgar (Figure 4).

In view of the uniqueness of the reaction mechanism, it seems auspicious to attempt an interpretation of the isomerization of realgar using some of the available kinetic models for solid-phase transitions. It should be borne in mind, however, that the mechanism of this reaction is a complex one (eqs 1−4), so the commonly employed solid-state kinetic models can be expected only to approximate the real kinetic law. To model the Raman and XRD decay curves, we tested the Johnson−Mehl−Avrami−Kolmogorov (JMAK)[22] and Prout−Tompkins (PT)[23] models (see Table S6 in the SI). When it was applied to the Raman data, the JMAK model, which is consistent with a variety of solid-state (including photo-induced) processes,[6,24−26] and has already been utilized to model the kinetics of realgar transformation followed by powder XRD,[13] reproduced reasonably well ($R^2 = 0.972$) only the kinetic curve at the lowest excitation density (0.11 mW cm^{-2}; Figure 1b). The progressively worse fits observed at higher excitation densities (Figure S2 and Table S6) indicated increased contribution from the light-stage reaction (facilitated by the visible probe beam under such conditions), which became more apparent by the improved double-exponential fit to two processes with comparable kinetics.[24] Conversely, the XRD experiment provided conditions for fairly independent analytical treatment of the dark and light reaction stages. Accordingly, the $V-t$ function[27] for mode 1, where the light stage predominated, conformed excellently to the JMAK formalism ($R^2 = 0.992$; Figure S3), affording rate constant $k = 7.4(2) \times 10^{-6}$ s^{-1}. In mode 2, however, the kinetic curve clearly adopted a quasi-sigmoidal shape (see the inset in Figure 2); thus, the reaction deceleration implied by the JMAK model was not suitable, and in fact, the autocatalytic (accelerating) PT model performed slightly better ($R^2 = 0.889$ vs 0.849), although the rate constants were on the same order [$k = 7.5(8) \times 10^{-6}$ vs $2.9(2) \times 10^{-6}$ s^{-1} (Figure S3)]. Although the PT model is clearly an oversimplification of the reaction mechanism described by eqs 1−4, this result conforms to the collective autocatalytic mechanism suggested for the dark stage of the reaction.

Acknowledgment. We thank the JST Agency (P.N.) and MASA (G.J.) for financial support, Prof. T. Stafilov for the ICP−AES analysis, Dr. M. Kochunnoonny for recording the UV−vis spectra, and the anonymous reviewers for the very constructive comments.

Supporting Information Available: Movies of the difference electron density, Raman spectra, kinetic plots, and zip files containing CIFs. This material is available free of charge via the Internet at http://pubs.acs.org.

References

(1) (a) Ohashi, Y. *Acta Crystallogr.* **1998**, *A54*, 842. (b) Raithby, P. R. *Crystallogr. Rev.* **2007**, *13*, 121. (c) Cole, J. M. *Acta Crystallogr.* **2008**, *A64*, 259.
(2) (a) Collet, E.; Lemée-Cailleau, M.-H.; Buron-Le Cointe, M.; Cailleau, H.; Wulff, M.; Luty, T.; Koshihara, S.; Meyer, M.; Toupet, L.; Rabiller, P.; Techert, S. *Science* **2003**, *300*, 612. (b) Techert, S.; Zachariasse, K. A. *J. Am. Chem. Soc.* **2004**, *126*, 5593. (c) Techert, S.; Schotte, F.; Wulff, M. *Phys. Rev. Lett.* **2001**, *86*, 2030. (d) Neutze, R.; Wouts, R.; Techert, S.; Kirrander, A.; Davidson, J.; Kocsis, M.; Schotte, F.; Wulff, M. *Phys. Rev. Lett.* **2001**, *87*, 195508. (e) Busse, G.; Tschentscher, T.; Plech, A.; Wulff, M.; Frederichs, B.; Techert, S. *Faraday Discuss.* **2002**, *122*, 105. (f) Geis, A.; Block, D.; Bouriau, M.; Schotte, F.; Techert, S.; Plech, A.; Wulff, M.; Trommsdorff, H. P. *J. Lumin.* **2001**, *94*, 493. (g) Coppens, P.; Zheng, S.-L.; Gembicky, M. *Z. Kristallogr.* **2008**, *223*, 265. (h) Kim, C. D.; Pillet, S.; Wu, G.; Fullagar, W. K.; Coppens, P. *Acta Crystallogr.* **2002**, *A58*, 133. (i) Coppens, P. *Faraday Discuss.* **2002**, *122*, 1. (j) Šrajer, V.; Teng, T.-y.; Ursby, T.; Pradervand, C.; Ren, Z.; Adachi, S.; Schildkamp, W.; Bourgeois, D.; Wulff, M.; Moffat, K. *Science* **1996**, *274*, 1726.
(3) A *set* of chemical reactions is "collectively autocatalytic" if some of those reactions produce catalysts, causing the entire set of chemical reactions to be self-sustaining if an input of energy and reactant molecules is provided.
(4) (a) Riehl, W. J.; Krapivsky, P. L.; Rener, S.; Segre, D. *Quant. Biol.* **2009**, 1. (b) Bagyinka, C.; Oesz, J.; Szaraz, S. *J. Biol. Chem.* **2003**, *278*, 20624. (c) Farmer, J. D.; Kauffman, S. A.; Packard, N. H. *Physica D* **1986**, *22*, 50. (d) Kauffman, S. A. *J. Theor. Biol.* **1986**, *119*, 1.
(5) Hordijk, W.; Steel., M. *J. Theor. Biol.* **2004**, *227*, 451.
(6) Moré, R.; Busse, G.; Hallmann, J.; Paulmann, C.; Scholz, M.; Techert, S. *J. Phys. Chem. C* **2010**, *114*, 4142.
(7) Douglass, D. L.; Shing, C.; Wang, G. *Am. Mineral.* **1992**, *77*, 1266.
(8) Street, G. B.; Gill, W. D. *Phys. Status Solidi* **1966**, *18*, 601.
(9) Naumov, P.; Makreski, P.; Jovanovski, G. *Inorg. Chem.* **2007**, *46*, 10624.
(10) Kyono, A. *J. Photochem. Photobiol., A* **2007**, *189*, 15.
(11) Bonazzi, P.; Bindi, L.; Olmi, F.; Menchetti, S. *Eur. J. Mineral.* **2003**, *15*, 283.
(12) Kyono, A.; Kimata, M.; Hatta, T. *Am. Mineral.* **2005**, *90*, 1563.
(13) Ballirano, P.; Maras, A. *Eur. J. Mineral.* **2006**, *18*, 589.
(14) Bonazzi, P.; Bindi, L.; Pratesi, G.; Menchetti, S. *Am. Mineral.* **2006**, *91*, 1323.
(15) Although latent light-induced defect sites can never be entirely excluded, the aging of the sample in the dark (several months to years), the exclusion of visible light and use of filtered ($\lambda > 660$ nm) light during the experiments, and the absence of saturation of the photoyield at increased excitation densities (Figure 1b) consistently disfavor significant contributions from such defects to the reaction. Moreover, to avoid contributions from any long-lived light-induced centers, in all of the measurements we used samples separated from the interior of larger crystalline blocks of the genuine material. Photoconductivity measurements on realgar crystals (see ref 8) have shown that the creation of a very small number of photocarriers occurs at ~2.07 eV (600 nm), which is away from the main energy gap at 2.40 eV (516 nm). At 2.07 eV, absorption of realgar is significant, albeit very small. Thus, any stray incident light would be additionally filtered in the interior of the crystals, which further decreases the possibility of trapping light centers.
(16) Genuine realgar crystals were collected from the Allchar mine (Macedonia). The purity of the samples of the same specimen from which crystals for XRD had been separated was confirmed by trace element analysis with

ICP−AES (for details, see the SI). Consistent with the results obtained previously for other specimens from the same mine using ETAAS and k_0−INAA (see: Stafilov, T.; Angelov, N.; Jaćimović, R.; Stibilj, V. *Microchim. Acta* **2005**, *149*, 229), the content of impurities in our realgar sample was typically in the ppm range, the highest being those of Fe (0.02731%), Ca (0.01547%), and Mg (0.00298%). At this level, the impurities are not expected to contribute significantly to the main photochemical reactions, which typically proceed with high yields and even to completion after long-term photoexcitation.

(17) (a) Trentelman, K.; Stodulski, L.; Pavlosky, M. *Anal. Chem.* **1996**, *68*, 1755. (b) Muniz-Miranda, M.; Sbrana, G.; Bonazzi, P.; Menchetti, S.; Pratesi, G. *Spectrochim. Acta* **1996**, *A52*, 1391.

(18) At 2.33 eV, energies of >0.02 mW cm^{-2} decreased the crystallinity of 30−60 μm crystals in <24 h, and energies of ∼0.5 mW cm^{-2} caused complete degradation in <0.5 h. In mode 1, 11 datasets were collected in 5 days before complete disintegration of the crystal occurred. In mode 2, 31 datasets were collected in the dark within 8 days (see the SI). To assess the effects of long-term exposure to X-rays on the crystal quality, 24 control datasets were also collected during 6 days on a nonexcited, light-protected crystal.

(19) Mullen, D. J. E.; Nowacki, W. *Z. Kristallogr.* **1972**, *136*, 48.

(20) Bindi, L.; Popova, V.; Bonazzi, P. *Can. Mineral.* **2003**, *41*, 1463.

(21) Bonazzi, P.; Menchetti, S.; Pratesi, G. *Am. Mineral.* **1995**, *80*, 400.

(22) The JMAK model is based on the equation $X(t) = 1-\exp[-(kt)^n]$, where $X(t)$ is the transformed fraction, t is the elapsed time from the start, k is the rate constant, and n is the Avrami exponent, a quantity related to the dimensionality of the reaction. See: (a) Johnson, W. A.; Mehl, R. F. *Trans. Am. Inst. Min. Metall. Pet. Eng.* **1939**, *135*, 416. (b) Avrami, M. *J. Chem. Phys.* **1941**, *9*, 177. (c) Avrami, M. *J. Chem. Phys.* **1940**, *8*, 212. (d) Avrami, M. *J. Chem. Phys.* **1939**, *7*, 1103. (e) Kolmogorov, A. N. *Bull. Acad. Sci. USSR, Phys. Ser.* **1937**, *1*, 335.

(23) The PT model is based on the equation $\alpha(t) = \{1 + \exp[-k(t- t_0)]\}^{-1}$, where $\alpha(t)$ is the transformed fraction, t is the elapsed time from the start (at $t = t_0$, $\alpha = 0.5$), and k is the rate constant. See: (a) Prout, E. G.; Tompkins, F. C. *Trans. Faraday Soc.* **1944**, *40*, 488. (b) Brown, M. E. *Thermochim. Acta* **1997**, *300*, 93.

(24) Bogadi, R. S.; Levendis, D. C.; Coville, N. J. *J. Am. Chem. Soc.* **2002**, *124*, 1104.

(25) Destro, R.; Ortoleva, E.; Soave, R.; Loconte, L.; Presti, L. L. *Phys. Chem. Chem. Phys.* **2009**, *11*, 7181.

(26) (a) Bertmer, M.; Nieuwendaal, R. C.; Barnes, A. B.; Hayes, S. E. *J. Phys. Chem. B* **2006**, *110*, 6270. (b) Benedict, J. B.; Coppens, P. *J. Phys. Chem. A* **2009**, *113*, 3116.

(27) It should be noted that the solid-state kinetic models such as those utilized here usually correlate the *conversion extent* (or a quantity proportional to it, such as the relative Raman band intensity employed here) with the reaction rate. However, because of the unavailabilty of such a quantity in our XRD experiment, where the conversion yield was not readily accessible, the change of the *relative volume* was considered in the analysis. As has been already pointed out elsewhere,[25] while this may be very useful, such an assumption may not always be entirely justified.

JA1030672